



## Research article

# Mechanism study of BMSC-exosomes combined with hyaluronic acid gel in the treatment of posttraumatic osteoarthritis

Xianqiang Liu, Yongshuai Chen, Tao Zhang\*

Beichen District Hospital of Traditional Chinese Medicine, China

## ARTICLE INFO

## Keywords:

BMSC-Derived exosomes  
HA  
PTOA  
Oxidative stress  
Anterior cruciate ligament resection alone

## ABSTRACT

**Objective:** To explore the mechanism and efficacy of gel in the treatment of posttraumatic osteoarthritis (PTOA), combined with hyaluronic acid (HA) and bone marrow mesenchymal stem cell exosomes (BMSC-EXOs), and to explain its role in alleviating oxidative stress damage induced by mitochondrial reactive oxygen species (ROS).

**Methods:** How is the therapeutic potential of toa influenced by bone marrow mesenchymal stem cells-EXO to be evaluated both in vitro and in vivo. In vitro, BMSC-EXOs were extracted and characterized from rat specimens and labeled with Dil. Rat primary chondrocytes were then isolated to create a cellular PTOA model. BMSC-EXOs + HA group, BMSC-EXOs + HA + 740Y-P group, model group, BMSC-EXOs group, HA group, and control group were included in the cell group, and the function of cartilage matrix and the level of oxidative stress could be evaluated. Cartilage matrix integrity and oxidative stress can be assessed by grouping rats. At the same time, a rat model of ptosis can be established by excision of the anterior cruciate ligament, and joint rehabilitation, with pro-inflammatory and Enzyme-linked immunosorbent assay (ELISA) can be used to determine anti-inflammatory markers.

**Result:** sThe combined use of BMSC-EXOs and HA gel was found to significantly reduce oxidative stress in chondrocytes and PTOA rat models, improving cartilage mechanical properties more effectively than BMSC-EXOs alone.

**Conclusion:** BMSC-EXOs combined with HA gel offer a promising treatment for PTOA by modulating damage caused by mitochondrial ROS-induced oxidative stress.

## 1. Introduction

Types of osteoarthritis include post-traumatic osteoarthritis, which occurs after a joint injury, such as intra-articular fractures, ligament injuries, or other joint traumas [1]. PTOA accounts for 12 % of OA cases, predominantly affecting younger individuals.

Shoulder instability, meniscus tears, patellar dislocation and dislocation are among the main risk factors [2].

The pathogenesis of PTOA involves disruption of cartilage matrix integrity due to oxidative stress, inflammatory reactions, cell death (apoptosis, necrosis, etc.), and ultrastructural changes in chondrocytes. Synovial inflammation encompasses mitochondrial dysfunction, oxidative and nitrosative stress, inflammatory reactions, and synovial macrophage infiltration. Subchondral bone changes involve uncoupling of bone remodeling, decreased bone formation, fibrosis, and increased bone tissue destruction [3–5]. NF-κB plays an important role in the regulation and activation of inflammatory response [6–8]. p38 and ERK MAPKs were strongly

\* Corresponding author. 436 Beijing-Tianjin Road, Beichen District, Tianjin, 300499, China.  
E-mail address: [zhangtao920000740@163.com](mailto:zhangtao920000740@163.com) (T. Zhang).

<https://doi.org/10.1016/j.heliyon.2024.e34192>

Received 2 February 2024; Received in revised form 3 July 2024; Accepted 4 July 2024

Available online 5 July 2024

2405-8440/© 2024 Published by Elsevier Ltd. This is an open access article under the CC BY-NC-ND license (<http://creativecommons.org/licenses/by-nc-nd/4.0/>).

associated with the spread of cartilage degeneration after injury and suggest that blocking their activities may decrease the risk of PTOA by upregulating expressions of MMP-13, ADAMTS-5, and TNF- $\alpha$  [9,10]. The inhibition of Jnk, along with the reduction of CCL2 and 7, significantly ameliorates gait parameters in PTOA mice, indicating pain relief associated with OA [11]. After injury, activation of male IL-6  $-/-$  mice with downstream mediators STAT3 and ERK was decreased in the knee joint and dorsal root ganglion (DRG). Janus kinase (JAK) is crucial in STAT and ERK signaling pathways in cartilage breakdown metabolism and transmitting DRG pain signals in tissue grafts [12]. The Wnt/ $\beta$ -catenin signaling pathway exhibits hyperactivity within the synovium of PTOA, influencing chondrocyte phenotype expression and proliferation [13]. The prognosis of pta can inhibit and improve inflammation through the regulation of CHI3L1 [14]. While the underlying pathogenesis is understood, low levels of reactive oxygen species (ROS) can be produced by nicotinamide adenine dinucleotide phosphate (NADPH) oxidase, and the progression of pta can be prevented by early intervention. Intracellular signal transduction is involved in articular chondrocytes, thereby maintaining cartilage homeostasis and regulating extracellular matrix (ECM) and chondrocyte proliferation and synthesis [15]. Compared to normal chondrocytes, ROS induced DNA damage was generated by OA chondrocytes, resulting in more severe ROS [16]. In synovial fluid, the main enzyme for ROS production is NADPH oxidase, which can exacerbate joint oxidative stress and mediate the progressive degradation of cartilage in OA patients [17]. Excessive ROS levels can degrade matrix components by inhibiting matrix synthesis, hindering cell migration, and decreasing growth factor activity. Matrix metalloproteinases (MMPs) are activated due to high ROS levels, cartilage degradation is intensified, and cell death processes can be inspired [18].

Non-hematopoietic stem cells in bone marrow refer to bone marrow mesenchymal stem cells, and a variety of cell types can be differentiated. The vesicles secreted by cells are exosomes (EXOs), which play an important role when intercellular communication is regulated and a variety of physiology and pathology are involved [19–21].

BMSCs regulate immune responses and promote tissue repair and regeneration, presenting a potential treatment approach for PTOA. They positively impact PTOA by secreting anti-inflammatory factors, promoting chondrocyte proliferation, and inhibiting chondrocyte apoptosis. Therapeutic effects can be demonstrated by the secretion of extracellular vesicles (EVs) by bone marrow mesenchymal stem cells, which contain proteins, lipids, RNAs, and other bioactive molecules that influence recipient cell functions. BMSC-derived EVs, particularly those rich in microRNAs, possess potent anti-inflammatory and immunomodulatory properties, promoting cartilage repair and regeneration by modulating gene expression and signaling pathways. These EVs can directly act on joint tissues, reducing inflammation and cartilage degradation, counteracting PTOA progression [22].

The key component of synovial fluid is hyaluronic acid (HA), plays a vital role in preventing joint deterioration. HA synthesis may not occur in all osteoarthritis (OA) patients, hence its exogenous administration is recommended to reduce discomfort and slow joint attrition by inhibiting pro-inflammatory cytokine secretion, deterring apoptosis, and regulating fibrotic development. The therapeutic application of HA in PTOA includes a hydrogel compound of crosslinked HA and Dexamethasone (cHA-Dex) to inhibit chondrocyte apoptosis and alleviate early PTOA stages. Amobarbital, an agent that reduces oxidative damage and cartilage cell death, is incorporated within the crosslinked HA hydrogel matrix, presenting a novel approach to PTOA prevention [23,24].

30–150 nm is exosome size, and a key role in intercellular communication can be played by transporting biologically active entities—such as proteins, lipids, and RNA—to target cells. They offer numerous therapeutic advantages, including biocompatibility and low immunogenicity, decreasing the immune rejection's risk. Exosomes protect their cargo against biological degradation, enhancing stability and bioavailability of medicinal substances. Their precision targeting, thanks to specific molecular signatures, allows for bespoke delivery to afflicted tissues or cellular groups. Biological barriers can be crossed by exosomes, for example, the barrier of blood-brain, and modulate immune responses by transporting anti-inflammatory agents, positioning them as a forefront innovative therapeutic strategy to mitigate inflammation and tissue distress [25–29].

Exosome therapy encompasses several sophisticated methodologies: The supernatant was purified by cell culture and fluid exosomes isolation. engineering exosomes through genetic engineering or drug loading techniques; precise in vivo administration to targeted lesion sites via injection or alternative methods; and monitoring exosome-based therapies by using exosomes as biomarkers to track disease progression and treatment effectiveness. The cell-free therapeutic strategy of repair and tissue regeneration refers to exosome therapy [30–37].

The major challenge in clearing circulating exosomes and body fluids is to consistently release the target site. Exosomes can be cleared through the kidneys, with their size, surface charge, and composition influencing distribution and clearance rates. They may also be recognized and cleared by macrophages and neutrophils of the immune system. Chemical modification or surface engineering can enhance exosome stability and circulation time, reducing rapid clearance risk [38–40].

Hydrogels, known for their excellent biocompatibility and porous structure, are ideal vehicles for exosome delivery, significantly enhancing sustained exosome release. Hyaluronic Acid (HA) is commonly used to alleviate PTOA symptoms, aiding exosome stability and conservation. HA provides a protective sheath for exosomes, safeguarding their integrity and preventing premature disintegration or elimination. HA's interaction with cellular surface receptors, such as CD44, enhances targeted delivery of HA-enriched exosomes to specific cell populations, increasing their therapeutic potential. These modified exosomes are efficiently absorbed via receptor-mediated endocytosis, boosting intracellular uptake of pharmaceutical compounds or bioactive constituents. HA also influences immune response regulation in exosomes, modulating inflammation and immune cell polarization. In addition, through bioactive substances and transport growth factors, tissue repair and regeneration can be involved with hyaluronic acid, thus promoting the recovery of damaged tissues [41–43]. pta can be treated by BMSC-EXOs + HA, and the potential mechanism of action of the regimen can be explored.

## 2. Materials and methods

### 2.1. Isolation and BMSCs's cultivation

BMSCs were isolated using the bone marrow adherent technique. Sprague-Dawley rats at 2 weeks of age (10 rats/group, Beijing HFK Biotechnology Co., LTD.) were selected, 5 min was 75 % alcohol disinfection time, isoflurane overdose euthanasia. Dulbecco's Modified Eagle Medium (DMEM) allows the bone marrow to be rinsed, and single-cell suspensions can be converted from sterile straws. Both femurs can be dissected under sterile conditions and the blood can be flushed with Dulbecco's phosphate buffered saline (D-PBS) (D1040, Solarbio). Tissue fragments can be filtered through a 200-mesh sieve, and red blood cells can be cleaved by lysis buffer (Solarbio: R1010). 5 min was the centrifugation time of 1200 rpm, the supernatant was discarded, the cell suspension was cultured in T75 bottles (75 cm<sup>2</sup>/rat), the cells were incubated with 5 % CO<sub>2</sub> at 37 °C, and the medium was refreshed 48 h later. Three days was the cycle of cell passage once, and further experiments were identified.

### 2.2. BMSC-EXOs isolation, Identification, and Tracing staining

Exo can be isolated in BMSC media using the Wayen exosome isolation kit (H-Wayen: EIQ3-04001). The supernatant was collected and centrifuged at 3000×g for 15 min at 4 °C. 10 mL of the supernatant could be mixed with 5 mL of extractants and left for overnight at 4 °C. At 4 °C and 3000×g, 1 h was the time for the mixture to be centrifuged, and 1 ml of D-PBS was re-suspended by the remaining cells, centrifuged at 10,000×g for 10 min, centrifuged again at 4 °C, and the supernatant was discarded. exo was identified by the final supernatant, and the red fluorescence could be labeled by the tracer Dil (Beyotime Biotechnology: C1991S).

### 2.3. Construction of OA model and primary culture of rat chondrocytes

Trypsin-collagenase digestion was performed, and 4-week-old Sprague-Dawley rats (n = 10) were sampled from chondrocytes. The rats were euthanized and sterilized in 75 % alcohol for 5 min. Costal cartilage and knee joint was dissected under aseptic conditions, minced, and digested with 0.25 % trypsin (Solarbio: 9002-07-7) at 37 °C for 15–20 min. 0.2 % collagenase II (Gibco: 17101-015) was added, the supernatant was discarded and digested at 37 °C for 30–60 min. The resulting mixture was filtered through a 200-mesh sieve and centrifuged at 1200 rpm for 5 min. The cell pellet was resuspended in growth medium (88 % DMEM + 10 % EXO-FBS + 1 % ITS + 1 % PS) and cultured at 37 °C with 5 % CO<sub>2</sub>. The cell-induced OA model can be treated with 10 ng/mL IL-1β (MedChemeExpress: HY-P73900). Cells were divided into various treatment groups, including control, model, BMSC-EXOs, HA, BMSC-EXOs + HA, BMSC-EXOs + 740Y-P, and BMSC-EXOs + HA + 740Y-P. The BMSC-EXOs and HA concentrations were 40 μg/mL and 300 μg/mL, respectively. The Animal Ethics Committee of Beichen District Hospital of Traditional Chinese Medicine approved all procedures.

### 2.4. PTOA rat model Construction

56 is the number of Sprague-Dawley rats at the age of 4 weeks, including HA group, BMSC-EXOs + HA group, BMSC-EXOs + 740Y-P group, model group, and BMSC-EXOs group. Anterior cruciate ligament resection was performed under isoflurane anesthesia to induce PTOA. The control group underwent only skin incision and suturing. One week post-operation, rats were exercised twice daily. 100 μL gastric saline can be injected into the joints of the BMSC-EXOs group, and 100 μL gastric saline can be injected into the joints of the model group after 4 weeks. 10 mg/kg 740Y-P can be administered in the BMSC-EXOs + HA + 740Y-P and BMSC-EXOs + 740Y-P groups, and joint damage can be assessed using the OARSI scoring system over a continuous period of 12 weeks.

### 2.5. Coverslip Immunofluorescence assay

Chondrocytes were seeded at 1000 cells/coverslip (10 mm<sup>2</sup>) and incubated overnight. 10 % neutral formalin can hold the cells in place, permeabilized with 0.1 % Triton-100, and treated with 3 % hydrogen peroxide to inactivate catalase. Cells were blocked with 2 % BSA (Solarbio: A8020) for 2 h, Incubation of primary antibodies against tubulin can be used (1:400, Abcam: AB7291) and collagen II (1:200, Abcam: AB34712) overnight at 4 °C. The next day, cells were treated with secondary antibodies: Alexa Fluor® 488 anti-rabbit IgG (1:500, Abcam: ab150081) and Alexa Fluor® 594 anti-mouse IgG (1:500, Abcam: ab150116) for 1 h at room temperature. The medium containing dapi is where the cells are placed, which can be observed under a confocal laser microscope (Nikon A1HD25).

### 2.6. HE staining

The paraffin wax is hydrated and dewaxed. Sections are stained with hematoxylin (Beso: ba4097) for 4 min, washed, and treated with 1 % hydrochloric acid alcohol. After bluing in 1 % ammonia and washing, sections were stained with eosin (Beso: ba4095) for 30 s, washed, dehydrated, cleared, and mounted with neutral gum. Observations were made using a microscope (LECAI: DM750).

### 2.7. ELISA

Levels of IL-4, IL-6, TNF-A, and IL-10 can be detected by ELISA kit (R&D). Standards, controls, and samples were added to corresponding wells (100 μL each), and serum/plasma samples were first mixed with 50 μL of sample diluent.

2 h is the incubation time at room temperature, biotinylated antibodies (IL-6, TNF-A, IL-10, IL-4) (100  $\mu$ L/well) can be added, and the Wells can be rinsed with a washing buffer. incubated for 30 min, and washed. Streptavidin-HRP (100  $\mu$ L/well) was added, incubated for 30 min, and washed. Substrate solution was added, and the color will be stopped by using 100  $\mu$ L of stopping fluid, and

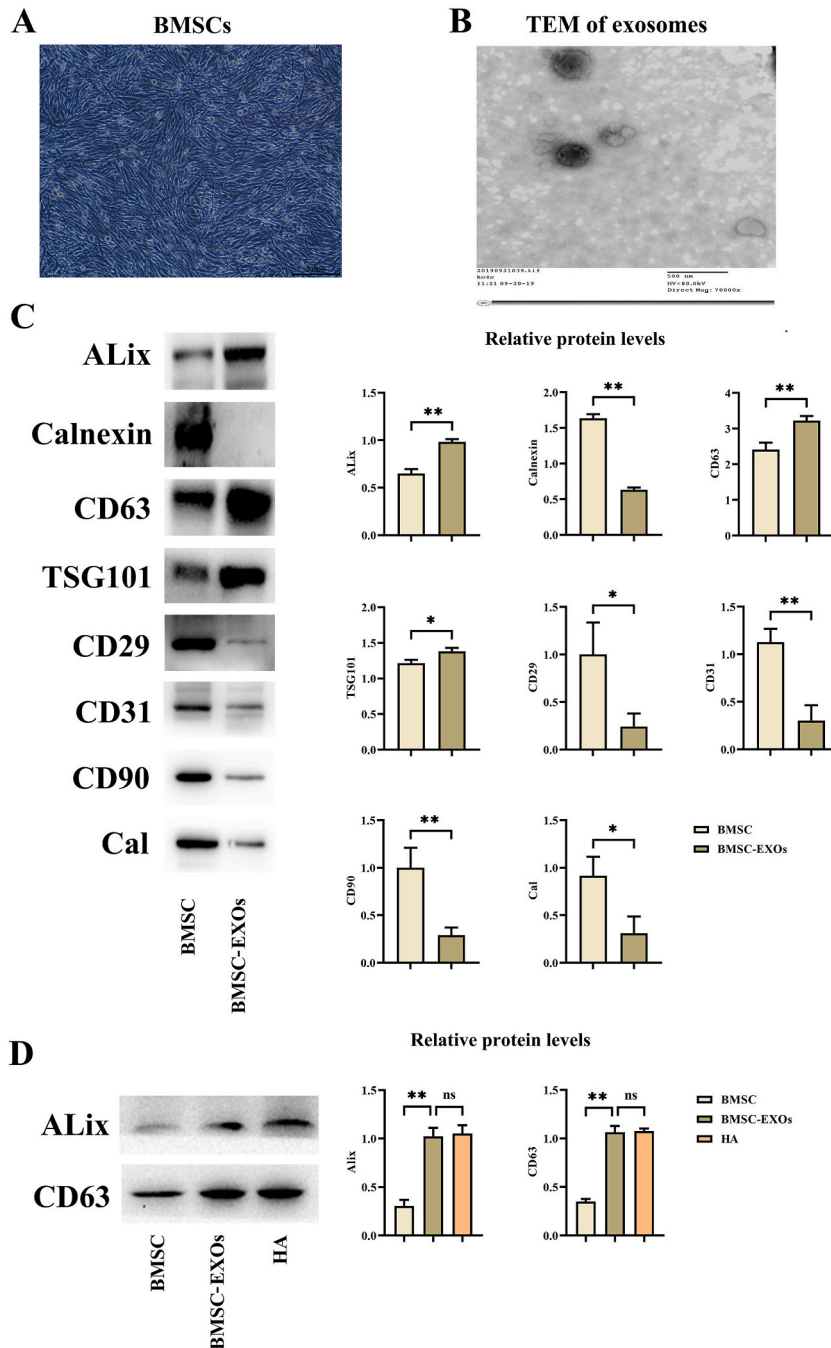


**Fig. 1.** Characterization of Bone Marrow-Derived Mesenchymal Stem Cell Exosomes (BMSC-EXOs). A: Microscopic imaging reveals BMSCs exhibiting a dense, spindle-shaped morphology under inverted microscopy. B: Through transmission electron microscopy, BMSC-EXOs are identified by their distinct cup-shaped morphology or hemispherical indentations. C: Western blot analysis confirms the significant presence of exosomal markers CD63, TSG101, and Alix, alongside the notable absence of the endoplasmic reticulum marker calnexin, indicating the purity and specificity of the extracted exosomes. The expressions of the markers CD29, CD31, and CD90 for BMSC were simultaneously assessed, yet the expression level of exosomes was notably low. D: Subsequent Western blot analysis delineates increased expressions of CD63 and Alix post-treatment with BMSC-EXOs + HA, underlining the bioactive effect of the treatment on exosomal marker expression. Significance levels are indicated as \* $p < 0.05$ ; \*\* $p < 0.01$ ; ns  $p > 0.05$ .

yellow can be changed from blue.

## 2.8. ROS Detection

Reactive Oxygen Species (ROS) are detected and DCFH-DA can be diluted in serum-free medium at a ratio of 1:1000, with 10  $\mu\text{mol/L}$  being the final concentration. After the cells are collected, the diluted DCFH-DA solution can be suspended by the cells, ensuring a cell density of one to two million cells per milliliter, and incubate at 37 °C for 20 min. During incubation, invert and mix every 3–5 min to ensure thorough interaction between the probe and the cells. The cells can be washed three times in serum-free medium after incubation, and unabsorbed DCFH-DA is removed. Cells can be stimulated by selected pharmacological agents as well as controls, or divide the cells into aliquots for different stimulations. Typically, a significant increase in reactive oxygen levels is observable 20–30 min after stimulation with the positive control. If the probe is loaded after cell collection, analyze the samples using a fluorescence spectrophotometer.

## 2.9. The assay of Western blotting

The protein concentration can be determined using the BCA protein assay kit (Solarbio: PC0020), and the total protein can be extracted from tissues and groups of cells. Add 5 $\times$  gel loading buffer proportionally, and heat the samples at 100 °C for 10 min. With 30  $\mu\text{g}$  of protein loaded per well, sodium dodecyl sulfate-polyacrylamide gel electrophoresis can be performed (SDS-PAGE) (stacking gel: 80 V for 40 min, separating gel: 110 V for 60 min). At 300 mah, the polyvinylidene fluoride (PVDF) film can be transferred from the isolated protein. Primary antibody can be incubated at 4 °C overnight, and 2 h is the time for blocking 5 % skim milk powder (OXOID: LP0031B), then wash the membrane.

1 h is the incubation time of the secondary antibody (Abcam: ab97080, 1:500 dilution) at room temperature, image development can be performed with the use of ECL kits, and statistical analysis can be performed.

Antibody	Dilution	Catalog Number	Manufacturer
Alix	1:2000	ab275377	Abcam
Calnexin	1:2000	ab22595	Abcam
CD63	1:2000	ab134045	Abcam
TSG101	1:2000	ab125011	Abcam
CollagenII	1:2000	ab307674	Abcam
MMP13	1:2000	ab315267	Abcam
gp91phox	1:2000	ab310337	Abcam
P22phox	1:2000	ab191512	Abcam
P47phox	1:2000	ab308256	Abcam
p-AKT	1:2000	ab308256	Abcam
T-AKT	1:2000	ab38449	Abcam
p-PI3K	1:2000	ab302958	Abcam
T-PI3K	1:2000	ab139307	Abcam

## 2.10. Statistical analysis

Mean  $\pm$  standard deviation ( $x \pm s$ ) was used to represent the data, and data analysis could be conducted through Prism 9.0 software. T-test could be used to analyze the difference between groups, and statistical significance could be shown when the P-value was less than 0.05. One-way analysis of variance could be used to compare between groups.

## 3. Results

### 3.1. Identification results of BMSC-EXOs

The morphology of exo can be extracted from rat bone marrow mesenchymal stem cell medium under electron microscope. EXOs were found to be cup-shaped or bi-concave, approximately 100 nm in diameter, with clear membrane boundaries (Fig. 1A and B). As can be seen from Western blotting results, CD63, TSG101 and ALIX in exo are highly expressed, while Calnexin, CD29, CD31 and CD90 are not expressed (Fig. 1C). Significant expression was found in HA as well as ALIX and CD63, while bmsc-exo was an isolated substance (Fig. 1D). The expression levels of CD29, CD31, and CD90 markers for BMSCs were also evaluated, showing a marked reduction in exosome expression.

### 3.2. How is BMSC-EXOs + HA affected by OA cartilage matrix synthesis and metabolism

Exo can be labeled by the tracer Dil, with which chondrocytes are co-cultured, and exo can be phagocytic by the discovery of chondrocytes, which also increases the amount of exo due to the development of time (8 h, 16 h, 24 h), and the source of chondrocytes is type II collagen and proteoglycan, while MMP13 is involved in ECM degradation. From a pta model stimulated by 10 ng/mL IL-1 $\beta$ ,

collagen II levels were reduced, and MMP13 levels were elevated. These trends were reversed by bmsc-exo and HA treatment, with the combined treatment showing superior results compared to individual treatments. There was no significant difference between the BMSC-EXOs + HA + 740Y-P group and the BMSC-EXOs +740Y-P group (Fig. 2B).

In the model group, The levels of pro-inflammatory factors IL-6 and  $\text{tnf-}\alpha$  were increased, while the levels of anti-inflammatory factors IL-10 and IL-4 were decreased. Both BMSC-EXOs and HA treatments reduced IL-6 and  $\text{TNF}\alpha$  levels and increased IL-10 and IL-4 levels. The combined treatment further enhanced these effects. The addition of 740Y-P reversed these trends, Statistical significance was not found between the BMSC-EXOs + HA + 740Y-P and BMSC-EXOs +740Y-P groups (Fig. 2C&D). ROS levels increased significantly in the model group. Treatments with BMSC-EXOs or HA reduced ROS levels, with a more pronounced effect in the combined treatment group. The addition of 740Y-P increased ROS levels in both the BMSC-EXOs and combined treatment groups, with no significant differences between them (Fig. 2E).

### 3.3. How is the level of ROS in osteoarthritis chondrocytes affected by BMSC-EXOs + HA

It is important that cartilage degeneration is affected by ROS, and inflammation and apoptosis of chondrocytes are triggered by

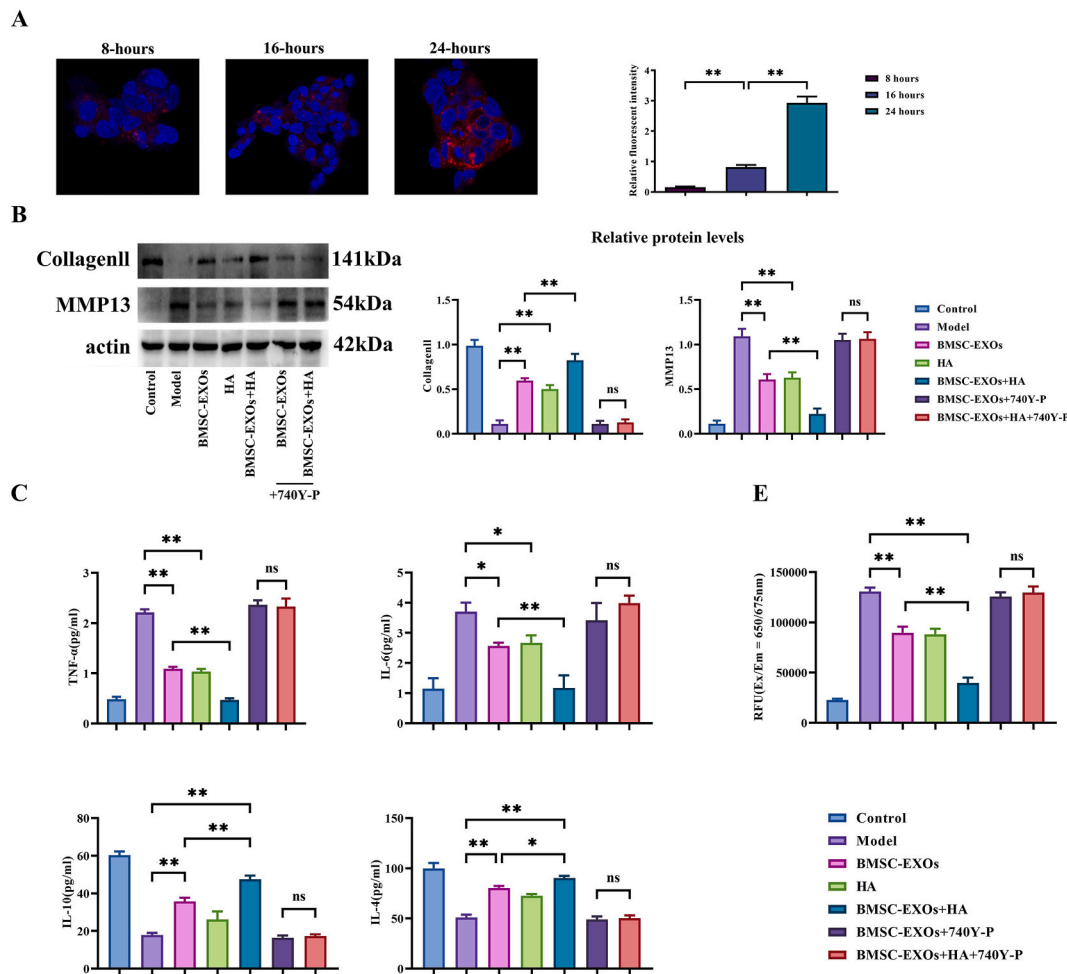


**Fig. 2.** Impact of BMSC-EXOs + HA on Osteoarthritis (OA) Cartilage Matrix Synthesis and Metabolism. A: Laser confocal microscopy at 600 × magnification exhibits time-dependent phagocytosis of BMSC-EXOs by chondrocytes over 8, 16, and 24 h. B: Treatment with BMSC-EXOs + HA is shown to enhance the synthesis of the extracellular matrix component, collagen II, while concurrently inhibiting the degradation marker, MMP13. Data resulted from triplicate experiments for enhanced reliability. C&D: Illustrated are the modulatory effects of BMSC-EXOs and HA treatments, both independently and combined, on the levels of pro-inflammatory (IL-6 and  $\text{TNF}\alpha$ ) and anti-inflammatory (IL-10 and IL-4) cytokines, before and after the application of 740Y-P. Treatments significantly adjust cytokine profiles favorably, this regulation is disrupted by 740Y-P, with no distinguishable difference between BMSC-EXOs and HA treatments post-740Y-P application. Significance markers as before. E : ROS detected the differential effects of BMSC-EXO, HA treatments, and their combination on ROS levels in a MODEL group, with a specific focus on the pronounced variations observed following the addition of 740Y-P. The comparative analysis underscores the distinct influence of single and combined therapeutic interventions on oxidative stress parameters.

high ROS levels. As chondrocytes were stimulated by  $il-1\beta$ , MDA levels and NADPH oxidase components were significantly increased, which decreased BMSC-EXOs treatment levels. The combined treatment showed a more evident reduction. The addition of 740Y-P negated these effects (Fig. 3A). Antioxidant system components SOD and GSH levels, reduced by IL-1 $\beta$ , after BMSC-EXOs treatment, with the combined treatment showing superior results. No significant differences were observed between the BMSC-EXOs + 740Y-P and BMSC-EXOs + HA + 740Y-P groups (Fig. 3B).

### 3.4. How is the PI3K/AKT signaling pathway in IL-1 $\beta$ -induced OA affected by BMSC-EXOs + HA

IL-1 $\beta$  can disrupt OA cell homeostasis by activating the pathway of PI3K/AKT. BMSC-EXOs treatment down-regulated PI3K/AKT phosphorylation, protecting damaged cells. This effect was more pronounced in the combined treatment group compared to individual treatments. Significant differences between groups could be eliminated by the addition of 740Y-P (Fig. 4), suggesting that BMSC-EXOs + HA may treat OA by regulating the PI3K/AKT pathway.

### 3.5. ROS level of pta model is decreased due to BMSC-EXOs + HA

From PTOA rat models, the articular cavity can be injected with BMSC-EXOs + HA and BMSC-EXOs. The level of MDA increased in the model group, while the level of SOD and GSH decreased. These changes were more pronounced in the combined treatment group compared to individual treatments. There was no significant difference between the BMSC-EXOs + HA + 740Y-P and BMSC-EXOs + 740Y-P groups (Fig. 5). These results indicate that ROS levels in pta models can be reduced by BMSC-EXOs + HA.

### 3.6. ECM synthesis can be promoted and inhibited by BMSC-EXOs + HA

The recovery ability of pta rat model was evaluated by HE staining, and the cartilage of control group had smooth and complete surface and neatly arranged cells, while the model group had obvious cartilage damage. Structural incompleteness was the characteristic of BMSC-EXOs group chondrocytes, while Relatively intact cartilages in the combined treatment group showed an increase in chondrocytes. The OARSI score indicated that BMSC-EXOs + HA improved chondrocyte proliferation (Fig. 6A). Western blotting showed reduced MMP13 and increased collagen II levels after BMSC-EXOs and combined treatment (Fig. 6B), indicating that collagen synthesis was promoted by BMSC-EXOs + HA, and degradation was inhibited.

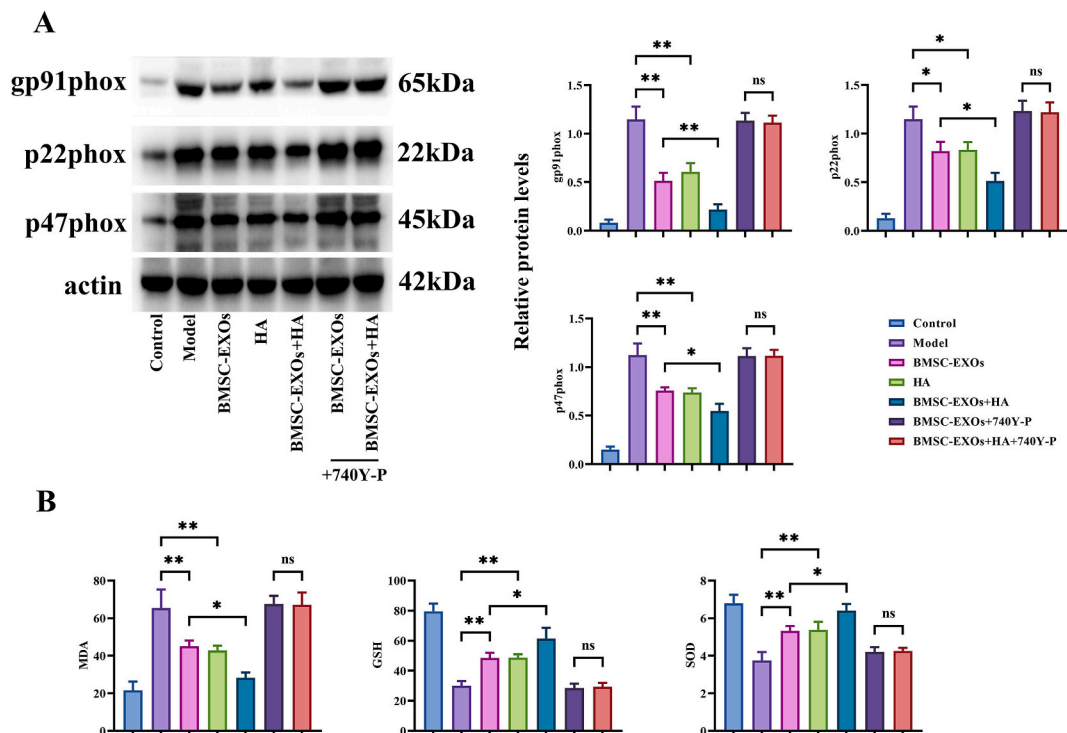


**Fig. 3.** BMSC-EXOs + HA Alleviates IL-1 $\beta$ -Induced Reactive Oxygen Species (ROS) Production in Chondrocytes. A: Western blot analysis quantifies the expression of NADPH oxidase subunits (p47phox, p22phox, and gp91phox), indicating ROS generation mechanisms. B: Cellular antioxidant status, represented through SOD and GSH levels, and lipid peroxidation marker, MDA, are evaluated, underpinning the antioxidative effects of the treatments. Analysis was repeated in triplicate for precision. Significance levels applied as previously noted.

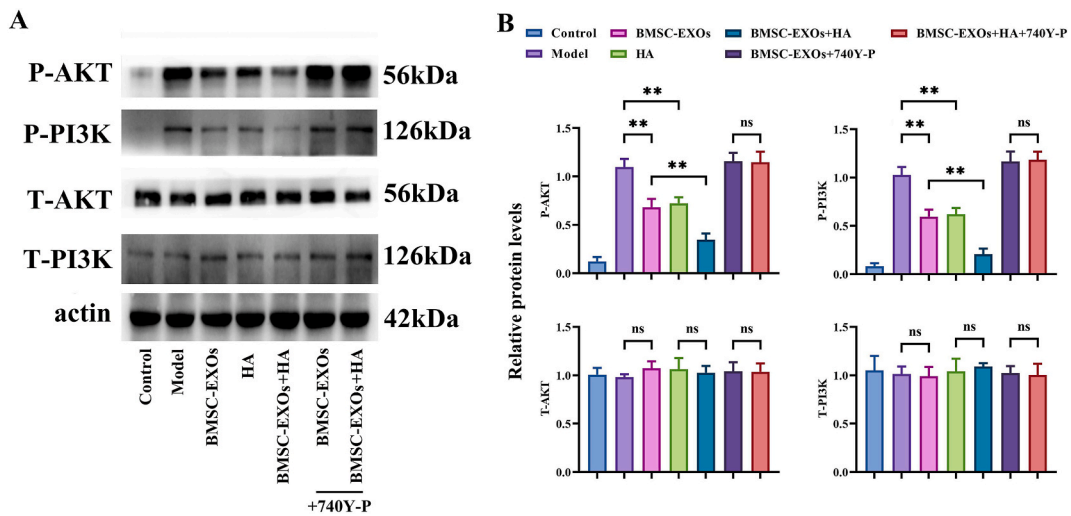


**Fig. 4.** Suppression of the PI3K/AKT Signaling Pathway Activation in OA by BMSC-EXOs + HA. A: Reduced levels of IL-1 $\beta$  and phosphorylation of PI3K/Akt signaling pathways elements highlight the treatment’s efficacy in modulating OA-related signaling. B: Quantitative analysis of Western blot bands provides statistical support for the observed effects, with the experiment being replicated three times for statistical rigor. Significance notations remain consistent.

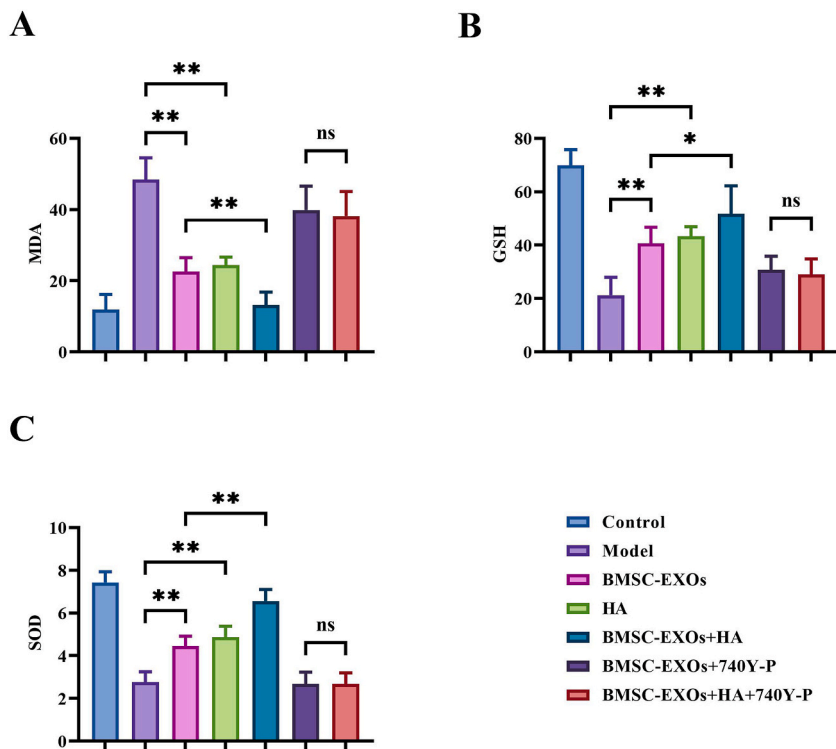


**Fig. 5.** Reduction of ROS Levels in a Rat Model of Post-Traumatic Osteoarthritis (PTOA) by BMSC-EXOs + HA. This presents the evaluation of ROS modulation in a PTOA model following BMSC-EXOs + HA administration, with detailed oxidative stress marker assessments (MDA, GSH, SOD) confirming the therapeutic potential of this approach. A group size of n = 8 ensured statistical relevance, with significance indicated as prior.

### 3.7. Schematic Diagram of BMSC-EXOs therapeutic process

The role of bone marrow mesenchymal stem cell-derived exosomes in toa therapy can be illustrated by this figure. Exosomes containing bioactive molecules are secreted and multiple cell types are differentiated by bone marrow mesenchymal stem cells. These



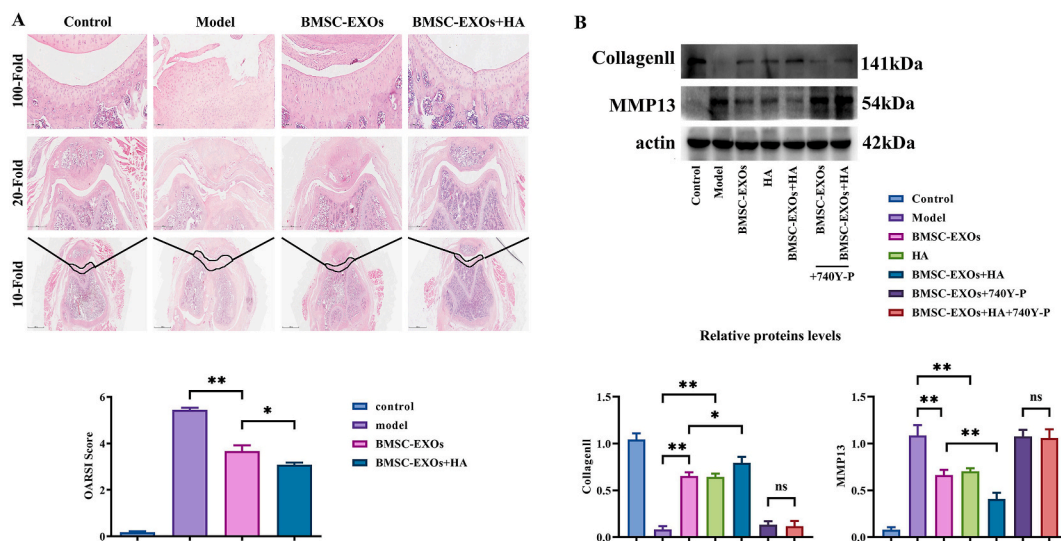


**Fig. 6.** BMSC-EXOs + HA's Role in Promoting Synthesis and Inhibiting Degradation of Chondrocyte Extracellular Matrix in a PTOA Model. \*\* Here, HE staining and OARSI scoring affirms tissue recovery, while Western blot assesses molecular changes in collagen II synthesis and MMP13 activity, showcasing the dual protective and restorative effects of the treatment. Group size and significance notation matched previous descriptions.

exosomes, delivered via hyaluronic acid gel, activate the PI3K/AKT pathway, modulate ROS levels, and suppress MMP13 activity, promoting collagen II synthesis. The hydrogel framework inhibits PI3K and AKT pathways, reducing oxidative stress and enhancing cartilage repair (Fig. 7). Western blot raw uncut strips in Supplementary file 1.

#### 4. Discussion

The diameter of 30–150 nm is BMSCS-EXO, small lipid membrane vesicles are secreted by BMSCs, and intercellular communication is mediated. They are captured by neighboring cells through ligand receptors or direct binding, facilitating information transmission [44].

Osteoblasts refer to bone marrow mesenchymal stem cells, and the repair of endogenous chondrocytes can be stimulated and damaged chondrocytes can be replaced, making them suitable for cartilage tissue repair. It can be seen from the study that the damaged tissue environment is regulated, a variety of nutritional factors are secreted by bone marrow mesenchymal stem cells, the cell regeneration process can be coordinated, differentiation, matrix synthesis, and cell proliferation are included. In addition, TGF- $\beta$ , MMPs and TIMPs are mediated by bone marrow mesenchymal stem cells, thereby reducing tissue damage and stimulating ECM synthesis, and inhibiting fiber remodeling and ECM degradation [45].

Cartilage lesions and treatment can be improved by bone marrow mesenchymal stem cells. Similar biological functions exist in bmsc and BMSC-EXO but are easier to store, can penetrate biofilms, and have low immunogenicity [46]. EXOs also do not proliferate, eliminating the risk of tumorigenesis [47]. As a long polysaccharide chain, cartilage and synovial fluid compose hyaluronic acid (HA), whose main functions are lubrication and shock absorption, thereby protecting joint structure and articular cartilage [48]. In the regulation of cell survival, proliferative, metabolic and inflammatory responses play an important role in the progression of pta. It protects and repairs chondrocytes, promoting their proliferation and migration, and inhibiting MMP13 expression, thus decelerating cartilage degradation. The pathway also modulates inflammatory reactions and oxidative stress responses, preserving chondrocyte integrity and inhibiting apoptosis through anti-apoptotic factors [49–51].

The PI3K/AKT signaling pathway was mediated by BMSC-EXOs in this study, and the generation of type II collagen in ECM was promoted and the degradation was inhibited in articular chondrocyte origin, significantly decreasing ROS levels in vivo, supporting BMSC-EXOs' role in OAtreatment. ROS, as a byproduct of cellular metabolism, regulate signaling transduction and redox equilibrium under normal conditions but trigger oxidative stress and damage under PTOA, contributing to cartilage matrix degradation and joint damage.

Reactive Oxygen Species (ROS) assume an essential and intricate role, This is particularly evident in the progression of post-traumatic osteoarthritis (pta). As a byproduct of cellular metabolism, ROS are associated with the regulation of signaling transduction and the redox equilibrium under standard physiological conditions. However, under the pathological circumstances of PTOA, an aberrant elevation in ROS levels triggers oxidative stress, which not only inflicts damage upon cell membranes, proteins, and DNA, fostering dysfunction and mortality in chondrocytes. The degradation of cartilage matrix is aided by the activation of enzymes, including A disintegrin, metalloproteinases, thromboreactive protein motifs (ADAMTS), and matrix metalloproteinases (MMPs), culminating in the disintegration of tissues. Furthermore, ROS, as a mediator of inflammation, amplifies inflammatory responses by activating the pathways of signaling like NF- $\kappa$ B, thus exacerbating joint damage and pain. The accumulation of ROS may also provoke

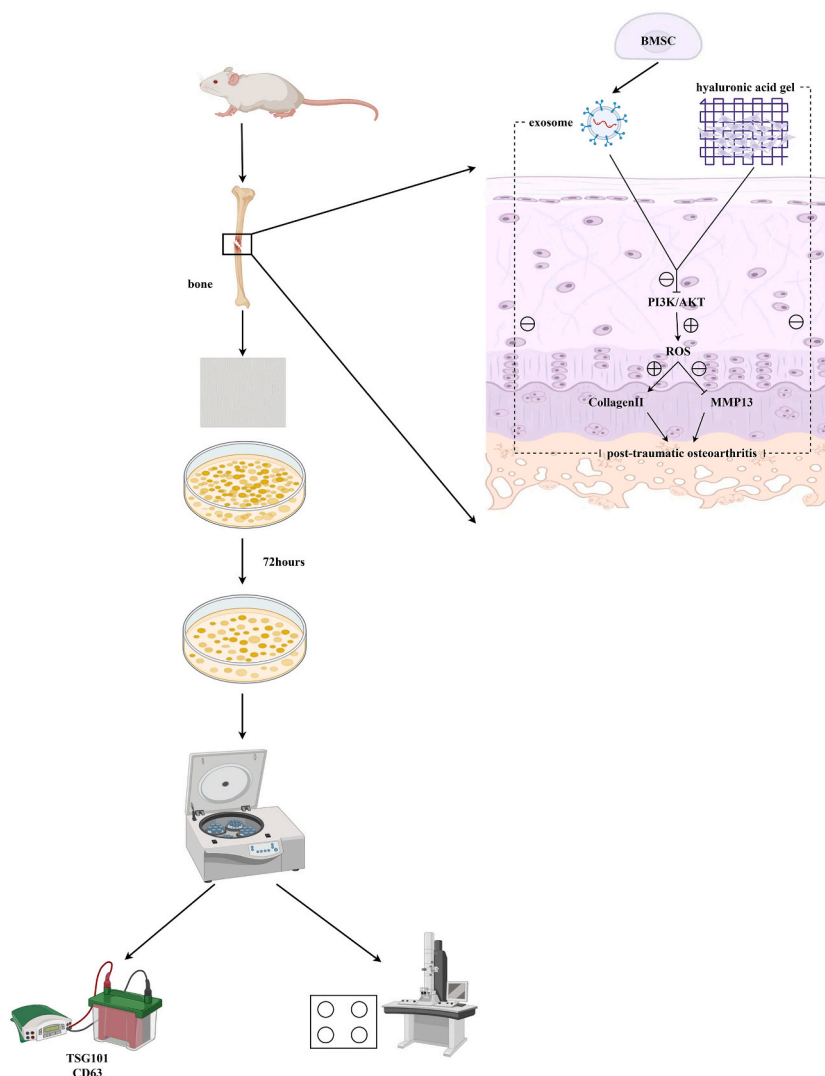


**Fig. 7.** Schematic Overview of BMSC-EXOs Delivered Through Hyaluronic Acid Gel in PTOA.

This illustration encapsulates the therapeutic mechanism wherein BMSC-EXOs, mediated via hyaluronic acid gel, activate PI3K/AKT signaling, modulate ROS levels, and regulate MMP13 activity, cumulatively fostering collagen II production and offering insight into the innovative treatment paradigm for post-traumatic osteoarthritis.

the apoptosis of chondrocytes via the mitochondrial pathway, a mechanism closely linked to the advancement of PTOA. Additionally, ROS's influence on autophagy and mitochondrial function, by affecting the dynamics of mitochondrial fusion and fission, interferes with cellular energy metabolism and viability, serving as a pivotal factor in the pathophysiology of PTOA [52–55]. Exosome extraction from cells typically yields limited amounts, challenging their clinical application due to complex and costly separation and purification processes. Optimizing extraction methods is necessary to improve efficiency and yield. Furthermore, the targeting precision of exosomes within the body is inadequate, potentially affecting therapeutic efficacy. Understanding the biological distribution and clearance mechanisms of exosomes is crucial for enhancing their therapeutic efficiency and safety. Variability in exosome functionality and stability across different samples and storage conditions necessitates further research for clinical application. Establishing standardized and scalable production processes is imperative for consistent and replicable exosome-based therapies [56,57].

Hyaluronic acid gel is commonly used for osteoarthritis treatment, but patients should be aware of potential adverse reactions, including local reactions like redness, pain, itching, or fever, which usually subside within a few days. More severe reactions like joint swelling, rashes, hives, difficulty breathing, infections, vascular damage, and joint stiffness require prompt medical attention [58,59].

Our study highlights the therapeutic potential of combining BMSC-EXOs and HA for treating PTOA. This combination significantly enhances type II collagen synthesis and reduces degradation, dramatically lowering ROS levels. The synergy between BMSC-EXOs and HA likely stems from HA's role as a joint lubricant and shock absorber, creating an optimal microenvironment for BMSC-EXOs' reparative functions. HA's involvement in ECM restoration and systemic ROS level reduction further supports chondrocyte recovery,

presenting a promising therapeutic approach for PTOA management.

In this study, OA can be regulated by the combination of exo and HA via the PI3K/AKT signaling pathway, offering a novel insight into their protective dynamics against OA pathogenesis. The co-administration of BMSC-EXOs and HA fosters cartilage restoration and ECM synthesis, mitigating PTOA's adverse effects on articular chondrocytes. However, our study's exploration of upstream signaling molecules is limited, necessitating further research and a full understanding of treatment mechanisms are needed.

The repair effect of bone marrow mesenchymal stem cell-EXO can be evaluated by using in vitro and in vivo models and HA on chondrocytes within a PTOA context. In vitro assays confirmed BMSC-EXOs' uptake by chondrocytes and IL-1 $\beta$ -induced ROS levels can be down-regulated through the PI3K/AKT signaling pathway, alongside increased collagen II production and ECM integrity. Corresponding in vivo assessments in a rat PTOA model corroborated these findings, showing enhanced ECM collagen II synthesis and reduced degradation, with the combined treatment outperforming BMSC-EXOs alone. As an innovative therapeutic approach, the potential of bone marrow mesenchymal stem cells-EXO and hyaluronic acid can be demonstrated through the results, marking significant progress in treating this debilitating condition.

### Ethics approval

The animal use protocol for this study has been reviewed and approved by the Beichen District Chinese Medicine Hospital Animal Experiment Ethics Committee.

### Data availability

The datasets generated during and/or analyzed during the current study are available from the corresponding author upon reasonable request.

### Financial resource

None.

### CRediT authorship contribution statement

**Xianqiang Liu:** Writing – review & editing, Writing – original draft, Methodology, Data curation. **Yongshuai Chen:** Writing – review & editing. **Tao Zhang:** Data curation.

### Declaration of competing interest

The authors declare that they have no known competing financial interests or personal relationships that could have appeared to influence the work reported in this paper.

### Acknowledgments

None.

### Appendix A. Supplementary data

Supplementary data to this article can be found online at <https://doi.org/10.1016/j.heliyon.2024.e34192>.

### References

- [1] A.C. Thomas, T. Hubbard-Turner, E.A. Wikstrom, et al., Epidemiology of posttraumatic osteoarthritis, *J ATHL TRAINING* 52 (6) (2016) 491–496, <https://doi.org/10.4085/1062-6050-51.5.08>.
- [2] J.E. Dilley, M.A. Bello, N. Roman, et al., Post-traumatic osteoarthritis: a review of pathogenic mechanisms and novel targets for mitigation, *BoneKey Rep.* 18 (2023) 101658, <https://doi.org/10.1016/j.bonr.2023.101658>.
- [3] L. Punzi, P. Galozzi, R. Luisetto, et al., Post-traumatic arthritis: overview on pathogenic mechanisms and role of inflammation, *RMD Open* 2 (2) (2016) e000279, <https://doi.org/10.1136/rmdopen-2016-000279>.
- [4] J.E. Dilley, M.A. Bello, N. Roman, et al., Post-traumatic osteoarthritis: a review of pathogenic mechanisms and novel targets for mitigation, *BoneKey Rep.* 18 (2023) 101658, <https://doi.org/10.1016/j.bonr.2023.101658>.
- [5] D. Mangiapani, J. Lewis, B. Furman, et al., Post-traumatic arthritis: an update the duke orthopaedic, *Journal* 3 (1) (2013) 32–35, <https://doi.org/10.5005/jp-journals-10017-1026>.
- [6] J.A. Bolduc, J.A. Collins, R.F. Loeser, Reactive oxygen species, aging, and articular cartilage homeostasis, *Free Radical Bio Med* 132 (2018) 73–82, <https://doi.org/10.1016/j.freeradbiomed.2018.08.038>.
- [7] O.M. Zahan, O. Serban, C. Gherman, et al., The evaluation of oxidative stress in osteoarthritis, *Med Pharm Rep* 93 (1) (2020) 12–22, <https://doi.org/10.15386/mpr-1422>.

- [8] J. Lieberthal, N. Sambamurthy, C.R. Scanzello, Inflammation in joint injury and post-traumatic osteoarthritis, *Osteoarthr Cartilage* 23 (11) (2015) 1825–1834, <https://doi.org/10.1016/j.joca.2015.08.015>.
- [9] W. Lu, J. Shi, J. Zhang, et al., CXCL12/CXCR4 Axis regulates aggrecanase activation and cartilage degradation in a post-traumatic osteoarthritis rat model, *Int. J. Mol. Sci.* 17 (10) (2016). PMID: 27690009.
- [10] L. Ding, E. Heying, N. Nicholson, et al., Mechanical impact induces cartilage degradation via mitogen-activated protein kinases, *Osteoarthr Cartilage* 18 (11) (2010) 1509–1517, <https://doi.org/10.1016/j.joca.2010.08.014>.
- [11] A. Pandey, M. Singla, A. Geller, et al., Targeting an inflammation-amplifying cell population can attenuate osteoarthritis-associated pain, *Arthritis Res. Ther.* 26 (1) (2024) 53, <https://doi.org/10.1186/s13075-024-03284-y>.
- [12] Y. Liao, Y. Ren, X. Luo, et al., Interleukin-6 signaling mediates cartilage degradation and pain in posttraumatic osteoarthritis in a sex-specific manner, *Sci. Signal.* 15 (744) (2022) eabn7082, <https://doi.org/10.1126/scisignal.abn7082>.
- [13] A.J. Knights, E.C. Farrell, O.M. Ellis, et al., Synovial fibroblasts assume distinct functional identities and secrete R-spondin 2 in osteoarthritis, *Ann. Rheum. Dis.* 82 (2) (2022) 272–282, <https://doi.org/10.1136/ard-2022-222773>.
- [14] Y. Song, D. Hao, H. Jiang, et al., Nrf2 regulates CHI3L1 to suppress inflammation and improve post-traumatic osteoarthritis, *J. Inflamm. Res.* 14 (2021) 4079–4088, <https://doi.org/10.2147/JIR.S310831>.
- [15] Y.E. Henrotin, P. Bruckner, J.P. Pujol, The role of reactive oxygen species in homeostasis and degradation of cartilage, *Osteoarthr Cartilage* 11 (10) (2003) 747–755, [https://doi.org/10.1016/s1063-4584\(03\)00150-x](https://doi.org/10.1016/s1063-4584(03)00150-x).
- [16] M.Y. Ansari, N. Ahmad, T.M. Haqqi, Oxidative stress and inflammation in osteoarthritis pathogenesis: role of polyphenols, *Biomed. Pharmacother.* 129 (2020) 110452, <https://doi.org/10.1016/j.biopha.2020.110452>.
- [17] W. Hou, C. Ye, M. Chen, et al., Excavating bioactivities of the enzyme to remodel the microenvironment for protecting chondrocytes and delaying osteoarthritis, *Bioact. Mater.* 6 (8) (2021) 2439–2451, <https://doi.org/10.1016/j.bioactmat.2021.01.016>.
- [18] N.P. Waters, A.M. Stoker, W.L. Carson, et al., Biomarkers are affected by impact velocity and maximum strain of cartilage during injury, *J. Biomech.* 47 (12) (2014) 3185–3195, <https://doi.org/10.1016/j.jbiomech.2014.06.015>.
- [19] J.A. Welsh, D.C.I. Goberdhan, L. O'Driscoll, et al., Minimal information for studies of extracellular vesicles (MISEV2023): from basic to advanced approaches, *J. Extracell. Vesicles* 13 (2) (2024) e12404, <https://doi.org/10.1002/jev2.12404>.
- [20] Y. Wang, M. Zhao, W. Li, et al., BMSC-derived small extracellular vesicles induce cartilage reconstruction of temporomandibular joint osteoarthritis via autotaxin-YAP signaling Axis, *Front. Cell Dev. Biol.* 9 (2021) 656153, <https://doi.org/10.3389/fcell.2021.656153>.
- [21] Y. Wang, J. Zhang, J. Li, et al., CircRNA\_014511 affects the radiosensitivity of bone marrow mesenchymal stem cells by binding to miR-29b-2-5p, *Bosnian J Basic Med.* 19 (2) (2019) 155–163, <https://doi.org/10.17305/bjbm.2019.3935>.
- [22] M.G. Rizzo, T.M. Best, J. Huard, et al., Therapeutic perspectives for inflammation and senescence in osteoarthritis using mesenchymal stem cells, mesenchymal stem cell-derived extracellular vesicles and senolytic agents, *Cells* 12 (10) (2023), <https://doi.org/10.3390/cells1210421>.
- [23] Z.W. Zhang, J.Y. Zhao, Y. Feng, et al., [Study on the mechanism of cross-linked hyaluronic acid-dexamethasone hydrogel in post-traumatic osteoarthritis], *Zhonghua Yixue Zazhi* 104 (9) (2024) 695–703, <https://doi.org/10.3760/cma.j.cn112137-20231008-00672>.
- [24] S. Periasamy, Y. Chen, D. Hsu, et al., Collagen type II solution extracted from supercritical carbon dioxide decellularized porcine cartilage: regenerative efficacy on post-traumatic osteoarthritis model, *Bioresour Bioprocess* 11 (1) (2024), <https://doi.org/10.1186/s40643-024-00731-1>.
- [25] M.A. Thomas, M.J. Fahey, B.R. Pugliese, et al., Human mesenchymal stromal cells release functional mitochondria in extracellular vesicles, *Front. Bieng. Biotechnol.* 10 (2022) 870193, <https://doi.org/10.3389/fbioe.2022.870193>.
- [26] J. Wan, Z. He, R. Peng, et al., Injectable photocrosslinking spherical hydrogel-encapsulated targeting peptide-modified engineered exosomes for osteoarthritis therapy, *J. Nanobiotechnol.* 21 (1) (2023) 284, <https://doi.org/10.1186/s12951-023-02050-7>.
- [27] R. Wang, W. Jiang, L. Zhang, et al., Intra-articular delivery of extracellular vesicles secreted by chondrogenic progenitor cells from MRL/MpJ superheater mice enhances articular cartilage repair in a mouse injury model, *Stem Cell Res. Ther.* 11 (1) (2020) 93, <https://doi.org/10.1186/s13287-020-01594-x>.
- [28] Q.F. Zhou, Y.Z. Cai, X.J. Lin, The dual character of exosomes in osteoarthritis: antagonists and therapeutic agents, *Acta Biomater.* 105 (2020) 15–25, <https://doi.org/10.1016/j.actbio.2020.01.040>.
- [29] J. Lu, Y. Zhang, X. Yang, et al., Harnessing exosomes as cutting-edge drug delivery systems for revolutionary osteoarthritis therapy, *Biomed. Pharmacother.* 165 (2023) 115135, <https://doi.org/10.1016/j.biopha.2023.115135>.
- [30] R. Tevlin, H. desJardins-Park, J. Huber, et al., Musculoskeletal tissue engineering: adipose-derived stromal cell implementation for the treatment of osteoarthritis, *Biomaterials* 286 (2022) 121544, <https://doi.org/10.1016/j.biomaterials.2022.121544>.
- [31] S.S.H. Tan, C.K.E. Tjio, J.R.Y. Wong, et al., Mesenchymal stem cell exosomes for cartilage regeneration: a systematic review of preclinical in vivo studies, *Tissue Eng Part B-RE* 27 (1) (2020) 1–13, <https://doi.org/10.1089/ten.TEB.2019.0326>.
- [32] H. Zhang, J. Huang, M. Alahdal, Exosomes loaded with chondrogenic stimuli agents combined with 3D bioprinting hydrogel in the treatment of osteoarthritis and cartilage degeneration, *Biomed. Pharmacother.* 168 (2023) 115715, <https://doi.org/10.1016/j.biopha.2023.115715>.
- [33] Y. Liang, X. Xu, X. Li, et al., Chondrocyte-targeted MicroRNA delivery by engineered exosomes toward a cell-free osteoarthritis therapy, *ACS APPL Mater Inter* 12 (33) (2020) 36938–36947, <https://doi.org/10.1021/acsami.0c10458>.
- [34] Z. Lin, Y. Wu, Y. Xu, et al., Mesenchymal stem cell-derived exosomes in cancer therapy resistance: recent advances and therapeutic potential, *Mol. Cancer* 21 (1) (2022) 179, <https://doi.org/10.1186/s12943-022-01650-5>.
- [35] Z.G. Zhang, B. Buller, M. Chopp, Exosomes - beyond stem cells for restorative therapy in stroke and neurological injury, *Nat. Rev. Neurol.* 15 (4) (2019) 193–203, <https://doi.org/10.1038/s41582-018-0126-4>.
- [36] K. Popowski, H. Lutz, S. Hu, et al., Exosome therapeutics for lung regenerative medicine, *J. Extracell. Vesicles* 9 (1) (2020) 1785161, <https://doi.org/10.1080/20013078.2020.1785161>.
- [37] B. Lu, J. Ku, R. Flojo, et al., Exosome- and extracellular vesicle-based approaches for the treatment of lysosomal storage disorders, *Adv. Drug Deliv. Rev.* 188 (2022) 114465, <https://doi.org/10.1016/j.addr.2022.114465>.
- [38] D.W. Hwang, M.J. Jo, J.H. Lee, et al., Chemical modulation of bioengineered exosomes for tissue-specific biodistribution, *Adv. Ther.* 2 (11) (2019), <https://doi.org/10.1002/adtp.201900111>.
- [39] N. Parada, A. Romero-Trujillo, N. Georges, et al., Camouflage strategies for therapeutic exosome evasion from phagocytosis, *J. Adv. Res.* 31 (2021) 61–74, <https://doi.org/10.1016/j.jare.2021.01.001>.
- [40] S. Lathwal, S.S. Yerneni, S. Boye, et al., Engineering exosome polymer hybrids by atom transfer radical polymerization, *P NATL ACAD SCI USA* 118 (2) (2021), <https://doi.org/10.1073/pnas.2020241118>.
- [41] D. Li, L. Gong, H. Lin, et al., Hyaluronic acid-coated bovine milk exosomes for achieving tumor-specific intracellular delivery of miRNA-204, *Cells* 11 (19) (2022), <https://doi.org/10.3390/cells11193065>.
- [42] K. Rilla, H. Siiskonen, M. Tammi, et al., Hyaluronan-coated extracellular vesicles—a novel link between hyaluronan and cancer, *Adv. Cancer Res.* 123 (2014) 121–148, <https://doi.org/10.1016/B978-0-12-800092-2.00005-8>.
- [43] W. Cui, S. Tie, M. Guo, et al., Engineering milk-derived exosome for enhancing cellular astaxanthin delivery, *J. Agric. Food Chem.* 70 (35) (2022) 10794–10806, <https://doi.org/10.1021/acs.jafc.2c03683>.
- [44] X. Chang, Z. Ma, G. Zhu, et al., New perspective into mesenchymal stem cells: molecular mechanisms regulating osteosarcoma, *J Bone Oncol* 29 (2021) 100372, <https://doi.org/10.1016/j.jbo.2021.100372>.
- [45] R. Zhang, J. Ma, J. Han, et al., Mesenchymal stem cell-related therapies for cartilage lesions and osteoarthritis, *Am J Transl Res* 11 (10) (2019) 6275–6289. PMID: 31737182.
- [46] M. Nawaz, F. Fatima, K.C. Vallabhaneni, et al., Extracellular vesicles: evolving factors in stem cell biology, *Stem Cells Int.* 2016 (2015) 1073140, <https://doi.org/10.1155/2016/1073140>.

- [47] A. Marote, F.G. Teixeira, B. Mendes-Pinheiro, et al., MSCs-derived exosomes: cell-secreted nanovesicles with regenerative potential, *Front. Pharmacol.* 7 (2016) 231, <https://doi.org/10.3389/fphar.2016.00231>.
- [48] V. Legré-Boyer, Viscosupplementation: techniques, indications, results, *Orthop Traumatol Surg Res* 101 (1 Suppl) (2015) S101–S108, <https://doi.org/10.1016/j.otsr.2014.07.027>.
- [49] X. Yao, J. Zhang, X. Jing, et al., Fibroblast growth factor 18 exerts anti-osteoarthritic effects through PI3K-AKT signaling and mitochondrial fusion and fission, *Pharmacol. Res.* 139 (2018) 314–324, <https://doi.org/10.1016/j.phrs.2018.09.026>.
- [50] T.H. Tseng, C.L. Chen, C.H. Chang, et al., IL-6 induces periostin production in human ACL remnants: a possible mechanism causing post-traumatic osteoarthritis, *J. Orthop. Surg. Res.* 18 (1) (2023) 824, <https://doi.org/10.1186/s13018-023-04308-0>.
- [51] S.M. Hwang, M. Feigenson, D.L. Begun, et al., Phlpp inhibitors block pain and cartilage degradation associated with osteoarthritis, *J ORTHOPAED RES* 36 (5) (2017) 1487–1497, <https://doi.org/10.1002/jor.23781>.
- [52] K.P. O'Grady, T.E. Kavanaugh, H. Cho, et al., Drug-free ROS sponge polymeric microspheres reduce tissue damage from ischemic and mechanical injury, *ACS Biomater. Sci. Eng.* 4 (4) (2017) 1251–1264, <https://doi.org/10.1021/acsbiomaterials.6b00804>.
- [53] M. Au, Z. Liu, L. Rong, et al., Endothelin-1 induces chondrocyte senescence and cartilage damage via endothelin receptor type B in a post-traumatic osteoarthritis mouse model, *OSTEOARTH CARTILAGE* 28 (12) (2020) 1559–1571, <https://doi.org/10.1016/j.joca.2020.08.006>.
- [54] C. Snider, D. Grant, S.A. Grant, Investigation of an injectable gold nanoparticle extracellular matrix, *J. Biomater. Appl.* 36 (7) (2021) 1289–1300, <https://doi.org/10.1177/08853282211051586>.
- [55] X. Yao, J. Zhang, X. Jing, et al., Fibroblast growth factor 18 exerts anti-osteoarthritic effects through PI3K-AKT signaling and mitochondrial fusion and fission, *Pharmacol. Res.* 139 (2018) 314–324, <https://doi.org/10.1016/j.phrs.2018.09.026>.
- [56] L. Han, Z. Zhao, C. He, et al., Removing the stumbling block of exosome applications in clinical and translational medicine: expand production and improve accuracy, *Stem Cell Res. Ther.* 14 (1) (2023) 57, <https://doi.org/10.1186/s13287-023-03288-6>.
- [57] Y. Lin, Y. Li, P. Chen, et al., Exosome-based regimen rescues endometrial fibrosis in intrauterine adhesions via targeting clinical fibrosis biomarkers, *STEM CELL TRANSL MED* 12 (3) (2023) 154–168, <https://doi.org/10.1093/stcltm/szad007>.
- [58] R.R. Bannuru, M.C. Osani, E.E. Vaysbrot, et al., OARSI guidelines for the non-surgical management of knee, hip, and polyarticular osteoarthritis, *OSTEOARTH CARTILAGE* 27 (11) (2019) 1578–1589, <https://doi.org/10.1016/j.joca.2019.06.011>.
- [59] F. Berenbaum, J. Grifka, S. Cazzaniga, et al., A randomized, double-blind, controlled trial comparing two intra-articular hyaluronic acid preparations differing by their molecular weight in symptomatic knee osteoarthritis, *Ann. Rheum. Dis.* 71 (9) (2012) 1454–1460, <https://doi.org/10.1136/annrheumdis-2011-200972>.